



# Analysis of the Spatial Changes and Influencing Factors of Landscape Patterns Along the Fujian-Guangdong Interconnection

Jianxun Zhang<sup>1</sup>, Guowei Chen<sup>2</sup>, and Chang Lu<sup>1</sup> (✉)

<sup>1</sup> Construction Branch of State Grid Fujian Electric Power Co., Ltd., Fuzhou 350011, China  
luchang\_fz@163.com

<sup>2</sup> State Grid Fujian Electric Power Co., Ltd., Fuzhou 350003, China  
chen\_guowei@fj.sgcc.com.cn

**Abstract.** The Fujian-Guangdong Power Grid Project is of significant importance for the research on the changes in landscape patterns and the impact factors on biodiversity along the Fujian-Guangdong interconnection line, as it is a key project in the national “14th Five-Year Plan” for power development. This study aims to combine forest disturbance observation to assess the extent of forest destruction and recovery along the line and to analyze the influencing factors of landscape patterns and biodiversity changes using relevant indices. We utilized the COLD algorithm to monitor forest disturbances and calculated three landscape indices, including patch number, largest patch index, and Shannon’s diversity index. We found that the power grid project has caused certain damage to the forests, but they have been able to recover within 3 to 4 months after construction completion. Through index analysis, we observed that a 1000-m buffer zone is most suitable for analyzing the landscape pattern around the power station. Furthermore, factors such as the power of wind turbines and the age classification of the surrounding forests have an impact on the landscape pattern. These findings can provide assistance for ecological conservation and restoration along the Fujian-Guangdong interconnection line, as well as serve as a reference for future environmental analysis of power grid projects.

**Keywords:** Forest Disturbance · Landscape Pattern · Forest Age

## 1 Introduction

On September 30, 2022, the key project of the national “14th Five-Year Plan” for power development, the Fujian-Guangdong Interconnection Project, was officially completed and put into operation [1]. This milestone signifies the first-ever interconnection of power grids between Guangdong and Fujian provinces. The project has significant implications for regional energy security, resource allocation, and the green transformation of energy. Spanning through Zhangpu, Yunxiao, and Pinghe counties in Zhangzhou City, within the province of Fujian, the project traverses diverse ecological landscapes, experiences variable climates, and possesses abundant biodiversity. Consequently, the study of landscape pattern variations and factors influencing biodiversity along the Fujian-Guangdong interconnection line holds significant scientific value and practical significance.

Forest disturbance detection is one of the essential means to study landscape ecology, utilizing multi-source remote sensing data for monitoring and management of forest cover changes [2]. It enables the detection and monitoring of forest disturbances by comparing changes between images captured at different time periods or through time-series change patterns. Landscape patterns refer to the spatial organization and distribution characteristics of surface landscape elements [3]. By analyzing landscape patterns, we can investigate the factors and mechanisms of spatial pattern changes along the construction of the Fujian-Guangdong Interconnection Project, and determine the characteristics of landscape evolution. Biodiversity encompasses the diversity of species, genes, and ecosystems [4]. The regions along the Fujian-Guangdong Interconnection Project exhibit abundant biodiversity.

In this study, we utilized Landsat and high-resolution satellite imagery to analyze the Fujian-Guangdong interconnection line. Employing the COLD algorithm, we monitored surrounding disturbances and observed the forest's degradation and recovery. Three landscape pattern indices, including patch count, were computed to analyze the changes in landscape patterns across different spatial scales. Additionally, the changes in three landscape pattern indices were also compared between different tower base power and different forest age structures. Subsequently, the influencing factors of the landscape pattern along the corridor were analyzed. Based on the results, we conducted an analysis of the ecological conditions along the line and provided assistance for subsequent ecological conservation efforts.

## 2 Data and Study Area

### 2.1 Study Area

The study area is located within the boundaries of Fujian Province and forms part of the Fujian-Guangdong interconnection power grid line, spanning approximately 70 km in length (Fig. 1). Geographically, it lies between 23°24'N and 25°15'N latitude, and 116°51'E to 118°08'E longitude. The area boasts a unique geographical position, characterized by diverse and complex topography, encompassing high mountains, hills, plains, and coastal regions. Within Fujian Province, the region traversed by the Fujian-Guangdong interconnection project mainly includes Zhangpu, Yunxiao, and Pinghe counties, all of which fall within the subtropical monsoon marine climate zone. This area exhibits a variety of ecological types, experiences diverse climatic changes, and boasts a rich biodiversity, abundant with plant and animal resources [5].

### 2.2 Data

In this study, Landsat 8 and Gaofen-1 imagery were employed as data sources for analysis, playing a crucial role in Earth observation and environmental monitoring. The Landsat 8 imagery is acquired by the joint operation of the National Aeronautics and Space Administration (NASA) and the United States Geological Survey (USGS) through the Landsat satellite series [6]. With a spatial resolution of 30 m, this study primarily utilized the red, green, blue, and near-infrared bands. The Gaofen-1 imagery belongs to

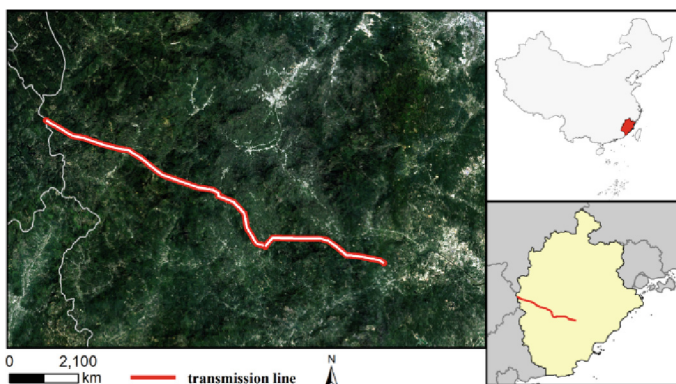


**Fig. 1.** The location of the study area. The red part in the picture is a part along the Fujian-Guangdong grid.

the High-Resolution Earth Observation Satellite series, launched by the China National Space Administration. Equipped with high-resolution optical sensors, the Gaofen satellite provides imagery data at a higher spatial resolution [7]. In this study, the Gaofen-1 imagery used had a resolution of 2 m, allowing for clearer observation of changes in the surrounding features of the tower base.

## 3 Methods

### 3.1 COLD Algorithm

The COLD (Continuous monitoring of Land Disturbance) algorithm is an enhanced algorithm used for land disturbance monitoring, which builds upon and improves the Continuous Change Detection and Classification (CCDC) algorithm [8]. It is designed to monitor various types of land disturbances. It offers several advantages over existing methods. Firstly, it provides high spatial (30 m) and temporal (up to four days) resolution automated accurate maps of land disturbance. Secondly, unlike many other disturbance algorithms that rely heavily on the availability of training data or inputs from several complicated algorithms, COLD detects land disturbance fully automated with Landsat time series as the only input data. This streamlined approach simplifies the process and improves efficiency. Thirdly, most of the rules and techniques used in COLD are based on ecological and biophysical processes that can be generalized for large areas and different kinds of environments. This generalizability enhances the algorithm's applicability and robustness. Lastly, with some adjustments (e.g., region-based thresholds), the COLD algorithm should have the capability of providing land disturbance maps for different regions. This flexibility further extends its utility in various geographical contexts.

The COLD algorithm primarily consists of three stages: data preparation, model initialization, and continuous monitoring. A normalized change vector magnitude is used as the threshold for change detection (Formula (1)). By continuously updating the model and observing new data, the COLD algorithm enables the continuous monitoring and extraction of land disturbances. With its optimized algorithmic workflow and rational

judgment criteria, the COLD algorithm effectively monitors various types of land disturbances, including subtle changes, thereby providing more accurate and comprehensive information on land changes.

$$\sum_{i=1}^k \left( \frac{\rho_i - \hat{\rho}_i}{RMSE_i} \right)^2 \sim \chi^2(k) > \chi_{0.99}^2 \quad (1)$$

where  $i$  is the  $i$ th band;  $k$  is Number of bands used for change detection;  $\rho_i$  is observed value for the  $i$ th band;  $\hat{\rho}_i$  is predicted value for the  $i$ th band.

### 3.2 Landscape Pattern Index

When assessing landscape pattern changes, landscape pattern indices are commonly used to characterize landscape fragmentation. In this study, three indices, namely patch number (N), largest patch index (LPI), and Shannon's diversity index (SHDI), were selected to describe landscape pattern changes. The N represents the total number of heterogeneous landscape elements in the landscape [9]. The LPI reflects the dominant patch types in the landscape, indirectly indicating the direction and magnitude of human-induced disturbances (Formula (2)) [10]. Shannon's diversity index is an important indicator of landscape heterogeneity, accurately identifying the spatial uneven distribution of different patch types in the landscape. A higher value indicates a more diverse land use and a more fragmented landscape (Formula (3)) [11].

$$LPI = \frac{Max(a_1, \dots, a_n)}{LA} \quad (2)$$

where  $a_n$  represents the area of the  $n$ th patch, and LA represents the total landscape area of the study area.

$$SHDI = - \int_{i=1}^n (p_i \ln p_i) \quad (3)$$

where  $p_i$  represents the proportion occupied by the landscape patch type  $i$ .

## 4 Results

### 4.1 Analysis of Forest Disturbance and Recovery

Based on high-resolution time-series remote sensing images, this study utilized the COLD algorithm to detect disturbance patterns around each tower base. Overall, within a  $1.5 \text{ km} \times 1.5 \text{ km}$  area surrounding each tower base, undisturbed areas were predominant, indicating the accuracy of the detection results. Regarding the disturbed areas, the largest extent of disturbance occurred during the construction phase of each tower base, aligning with the actual construction timeline. By combining the time-series imagery with the disturbance results, the analysis reveals that the forests in each area experienced three stages: pre-construction stability, forest disturbance during construction, and gradual recovery after construction completion. Furthermore, the extent of disturbance in each area exhibited varying patterns due to different construction conditions, operational status, and terrain characteristics.

We selected two representative regions for analysis, utilizing remote sensing imagery before and after the disturbance. In the first region, the northwestern part shows the disturbed area caused by construction activities (Fig. 2). By examining the extent of disturbance and the occurrence of disturbance events in this area, it can be observed that the construction of the tower base occurred in three stages. The first stage began in November 2021 with tree felling, followed by the second and third stages in February and March 2022, respectively. Based on the area of disturbance, it is evident that the third stage had the largest construction scope, with the disturbance trend gradually increasing from November 2021 and peaking in March 2022, followed by a decline indicating the start of recovery. Furthermore, due to a temporary suspension of construction activities and subsequent resumption the following year, the time span of disturbance in this area was prolonged. It is possible that vegetation, which had started to recover after the first stage, experienced repeated disturbance when construction activities resumed. Lastly, based on the post-construction remote sensing imagery, despite experiencing prolonged and multiple disturbances, some areas that experienced earlier disturbances (e.g., in November of the previous year) showed signs of vegetation greening and recovery by June 2022.

In the second region, combining the analysis with remote sensing imagery (Fig. 3), it can be observed that the central part of the area consists of scattered disturbed areas arranged horizontally from east to west. These point-like areas correspond to tower bases required for the construction of the power line. The disturbed areas are linearly aligned, following the alignment of the power line. Based on the occurrence time of disturbance in these areas, it is evident that several tower bases were disturbed simultaneously during the period from February to April 2022, suggesting synchronized construction with a relatively short duration. The disturbed areas are relatively small and generally consistent with the size of the tower bases. The terrain in this region exhibits minimal variation, making construction less challenging and allowing for a shorter construction period. Therefore, in the post-construction imagery from June 2022, it can be observed that the majority of the areas that underwent disturbance have already started to recover.

In conclusion, the forest disturbances within the study area exhibit various patterns influenced by construction conditions, difficulty, terrain, and other factors. Although the degree of disturbance, duration, and frequency of repetitions vary, resulting in varying degrees of damage to the forest, it is noteworthy that the majority of the areas begin to recover within 3 to 4 months after construction completion.

## 4.2 Changes in Landscape Pattern Across Different Spatial Scales

Tables 1–3 display the results of four indices calculated within buffer zones of 500 m, 1000 m, and 1500 m around the tower bases. The majority of tower base points show an increasing trend in the N index as the buffer zone expands. This is because as the range increases, the complexity within the area increases, resulting in a higher number of fragmented patches in the environment. Therefore, in larger buffer zones, the analysis includes a greater variety of land cover types and landscape features, leading to an increase in the N index. However, there are a few tower base points, such as 1#-P1 and 41#-P1 plots, that exhibit a decreasing trend followed by an increasing trend as the range expands. This is because, within the 1000-m range of these plots, the proportion

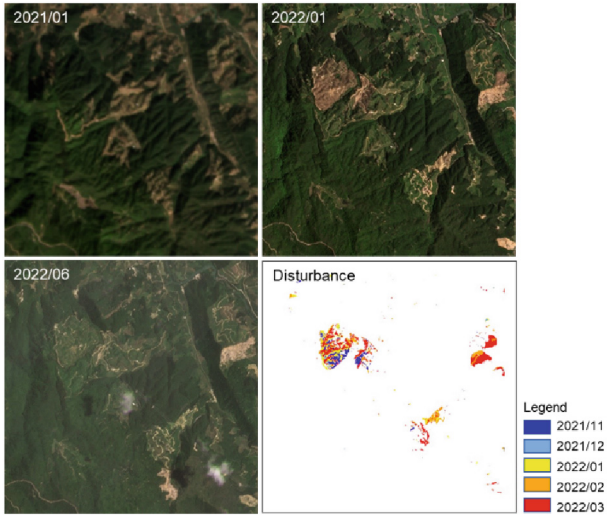


**Fig. 2.** Temporal imagery and disturbance map around the tower base (bottom right). From left to right, top to bottom: 2021/01 – no construction, 2022/01 – construction begins with disturbances, 2022/06 – construction completed and vegetation recovery initiates.

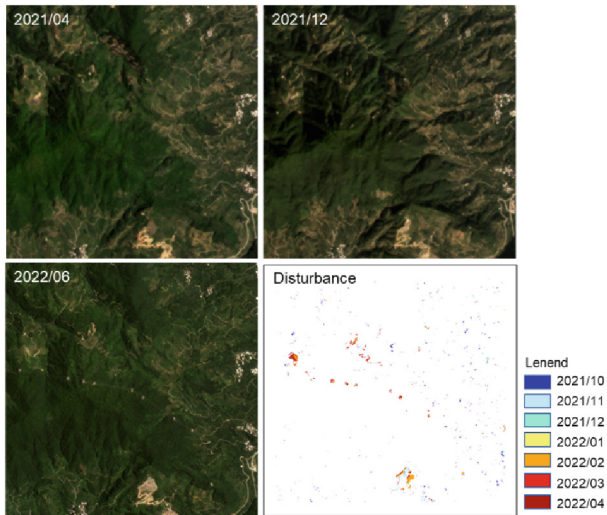


**Fig. 3.** Temporal imagery and disturbance map around the tower base (bottom right). From left to right, top to bottom: 2021/01 – no construction, 2022/01 – construction begins with disturbances, 2022/06 – construction completed and vegetation recovery begins.

of forests is higher and more concentrated. Thus, when the range expands from 500 m to 1000 m, these two indices decrease due to the inclusion of relatively fewer land cover types. However, when the range expands from 1000 m to 1500 m, the land cover types

become more complex and fragmented, resulting in an increase in the indices. This variation indicates that the differences in landscape features and land cover distribution within different tower base plots can lead to varying trends in the indices across different ranges.

The variation of the LPI and the SHDI does not exhibit a clear pattern compared to the first two indices. This is because the LPI is determined by the largest patch within each tower base, and the size of the index varies as the range expands due to the different largest patches in each area. Additionally, the LPI is also influenced by other factors such as landscape shape and layout. In contrast to the LPI, the SHDI depends on the location of the tower base. If the tower base is located at the edge of a town, the inclusion of the town will increase the SHDI as the range expands. This is because areas at the edge of towns typically have higher landscape heterogeneity, and as the range expands, a greater variety of land cover types enter the range, thereby increasing the landscape heterogeneity. Therefore, the variation of the maximum patch index and the SHDI may exhibit different patterns in different situations, depending on the location of the tower base and the characteristics of the surrounding landscape.

Based on the above analysis, it can be observed that when studying the spatial landscape pattern of tower bases, selecting a range that is too large can easily be influenced by factors outside the tower bases, such as urban areas, leading to distorted analysis results. On the other hand, choosing a range that is too small may overlook the influence of some tower bases on the surrounding environment, failing to capture the complete picture of these impacts and limiting a comprehensive understanding of the tower base landscape pattern. Therefore, using a 1000-m buffer zone around the tower bases as an appropriate spatial range for landscape pattern analysis is reasonable. This range takes into account the influence range of the tower bases themselves while avoiding excessive interference from non-tower base factors.

**Table 1.** Results of Four Indices within the 500-m Buffer Zone of Each Tower Base.

Tower Number	N	LPI	SHDI
1#-P1	401	0.020877747	1.589290704
41#-P1	411	0.015906553	1.520274484
45#-P1	359	0.011628534	1.77377741
46#-P1	400	0.013777854	1.768775916
49#-P1	356	0.016420486	1.572914525
50#-P1	337	0.018135183	1.526265123
51#-P1	411	0.013625577	1.617397436
1#-P1	432	0.014973859	1.617760735



**Table 2.** Results of Four Indices within the 1000-m Buffer Zone of Each Tower Base.

Tower Number	N	LPI	SHDI
1#-P1	354	0.011939432	1.573959316
41#-P1	405	0.022186374	1.543204838
45#-P1	393	0.021334577	1.770785108
46#-P1	468	0.012851505	1.754516155
49#-P1	389	0.015122963	1.630979635
50#-P1	379	0.009883699	1.610842823
51#-P1	439	0.010979773	1.56191216
1#-P1	434	0.011149497	1.625540084

**Table 3.** Results of Four Indices within the 1500-m Buffer Zone of Each Tower Base.

Tower Number	N	LPI	SHDI
1#-P1	372	0.014042752	1.513284449
41#-P1	414	0.018599944	1.592059453
45#-P1	377	0.016241244	1.767096902
46#-P1	465	0.008903419	1.741417489
49#-P1	369	0.012960954	1.682751152
50#-P1	366	0.02286686	1.659907154
51#-P1	461	0.021139473	1.600264799
1#-P1	443	0.011530189	1.60429509

### 4.3 Influence of Different Factors on the Landscape Pattern Along the Line

While the selection of spatial range indirectly affects the distribution of landscape patterns, there are other factors that directly impact the degree of landscape fragmentation. Based on While the selection of spatial range indirectly affects the distribution of landscape patterns, there are other factors that directly impact the degree of landscape fragmentation. Based on this, this study investigates the influence of tower base power and forest age structure on landscape patterns. We selected three different tower base power levels (110 kV, 220 kV, 500 kV) and calculated the changes in three landscape indices within a 1000-m buffer zone (Fig. 4). From the figure, it can be observed that both the number of patches and Shannon's diversity index increase with the increase in tower base power. However, the maximum patch index initially decreases and then increases with the increase in tower base power. This indicates that as the tower base power increases, the surrounding landscape becomes more fragmented, leading to greater disturbance. The reason for this may be that low-power tower bases have smaller land areas, and the



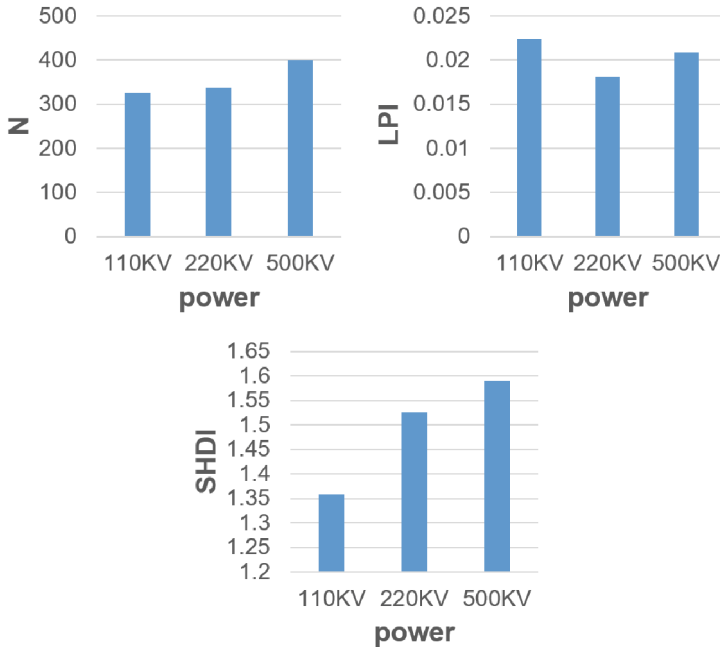


**Fig. 4.** Changes in landscape pattern indices around three different tower base power levels.

construction process involves minimal entry of large vehicles, resulting in lower vegetation disturbance. This study investigates the influence of tower base power and forest age structure on landscape patterns. We selected three different tower base power levels (110 kV, 220 kV, 500 kV) and calculated the changes in three landscape indices within a 1000-m buffer zone (Fig. 4). From the figure, it can be observed that both the number of patches and Shannon's diversity index increase with the increase in tower base power. However, the maximum patch index initially decreases and then increases with the increase in tower base power. This indicates that as the tower base power increases, the surrounding landscape becomes more fragmented, leading to greater disturbance. The reason for this may be that low-power tower bases have smaller land areas, and the construction process involves minimal entry of large vehicles, resulting in lower vegetation disturbance.

Two tower bases were selected with different surrounding forest age levels (average age of 15 years and 30 years), and the three landscape pattern indices for January 2021 and March 2023 were compared (Fig. 5), representing the period before and after the construction of the power project, respectively. From the figure, it can be observed that the number of patches decreases with higher forest age levels. The maximum patch index and Shannon's diversity index increase with increasing forest age during the period of maximum disturbance, but decrease with increasing forest age at the current stage. Areas with higher forest age levels tend to be densely wooded forest areas. Therefore, constructing power projects in these areas may be more challenging. Additionally, the recovery rate in these areas may be slower compared to areas with lower forest age,

possibly because mature forests take longer to recover from the damage caused by construction activities.

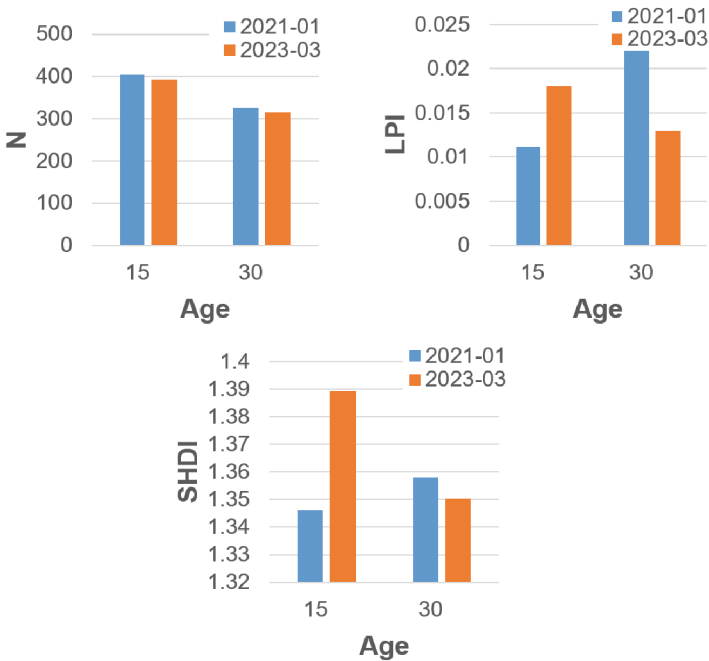


**Fig. 5.** Changes in three landscape pattern indices under different surrounding forest age levels.

## 5 Discussion

This study analyzed the forest disturbance around multiple tower sites and assessed the degradation and recovery of three forest regions. However, there are uncertainties associated with the forest disturbance results, primarily stemming from both the imagery and the algorithm used. In terms of imagery, we utilized high-resolution imagery from the GF-1 satellite [12]. However, variations in reflectance between adjacent images due to factors like clouds and sensor quality may lead to erroneous detection results. Despite selecting high-quality imagery data, these influences still persist. Additionally, we employed the COLD algorithm for forest disturbance monitoring, which has some limitations such as temporal lag and potential errors in threshold adjustments, leading to some degree of inaccuracy. Nevertheless, these errors have a minor impact on the final disturbance monitoring results and do not significantly affect the reliability of the findings. Therefore, despite the uncertainties and limitations associated with the imagery and algorithm, the results of this study still maintain a high level of credibility. We selected high-quality imagery data and employed a reliable disturbance monitoring algorithm to ensure the accuracy and reliability of the results. However, when interpreting and

discussing the results, it is important to acknowledge these uncertainties and limitations and provide appropriate discussions and explanations to better understand and interpret the research findings.

The power grid project has achieved good results in vegetation restoration, and the restoration will basically take 3–4 months. At the same time, the 1000-m buffer zone is most suitable for analyzing the landscape pattern around the power station, which takes into account the environment around the tower and can be applied to most power stations. The article also found that the power of wind turbines and the age class of surrounding forests can have an impact on landscape patterns and that for high-power and older forest environments, increased forest restoration efforts are needed. Taking different restoration measures according to the power of the power station and the surrounding environment can improve the restoration efficiency and contribute to the ecological restoration of the power grid project.

## 6 Conclusion

This study focused on a section of the Fujian province along the Fujian-Guangdong Interconnection Project as the research area. Based on high-resolution time-series remote sensing imagery, the COLD algorithm was used to detect disturbance maps at each tower site, enabling the analysis of forest degradation and recovery around the tower sites. Additionally, comparisons were made regarding landscape pattern changes at different spatial scales and the impact of various factors on landscape patterns. The following conclusions are drawn:

- (1) The electrical grid construction projects in the study area caused varying degrees of forest damage, but most areas began to recover within 3 to 4 months after construction completion.
- (2) Landscape pattern changes varied across different spatial scales, with the 1000-m buffer zone being the most suitable for analyzing landscape patterns around the power projects.
- (3) The power of wind turbines and the age class of surrounding forests can have an impact on the landscape pattern. Under different power and age class combinations, the extent to which the landscape pattern around wind turbines is affected varies. Higher turbine power results in a more fragmented landscape. Older surrounding forests take longer to recover the landscape pattern.

The results of this study indicate that although the Fujian-Guangdong Interconnection Project caused some degree of forest damage along the transmission lines, the forests have shown signs of recovery, likely due to the implemented restoration measures. The findings on landscape patterns and biodiversity not only provide valuable insights for the ecological restoration of the interconnection project but also serve as a reference for future power engineering projects. Therefore, this research holds scientific and practical value, contributing to both scientific understanding and guiding practices in the field.

**Author Contributions.** Methodology, Jianxun Zhang; software, Jianxun Zhang; validation, Guowei Chen and Chang Lu; formal analysis, Jianxun Zhang; data curation, Guowei Chen; writing – original draft preparation, Chang Lu. All authors have read and agreed to the published version of the manuscript.

**Funding.** This work is supported by the State Grid Fujian Electric Power Co., LTD (52130T220007).

**Conflicts of Interest.** The authors declare no conflict of interest. The funders had no role in the design of the study; in the collection, analyses, or interpretation of data; in the writing of the manuscript, or in the decision to publish the results.

## References

1. Ling, W., Ming, L., Fangjie, W.: Research on control strategy of canceling tap changer in back to back dc project. In: 10th Renewable Power Generation Conference, pp. 678–683 (2021)
2. Chen, X., Zhao, W.Z., Chen, J.G., Qu, Y., Wu, D.H., Chen, X.H.: Mapping large-scale forest disturbance types with multi-temporal CNN framework. *Remote Sens.* **13**(24), 5177 (2021)
3. Wu, Z.F., Wei, L.Z., Lv, Z.Q.: Landscape pattern metrics: an empirical study from 2-d to 3-d. *Phys. Geogr.* **33**(4), 383–402 (2012)
4. Syrbe, R.U., Michel, E., Walz, U.: Structural indicators for the assessment of biodiversity and their connection to the richness of avifauna. *Ecol. Ind.* **31**(5), 89–98 (2013)
5. Ma, Z.G., et al.: Recent changes in temperature and precipitation of the summer and autumn seasons over Fujian Province, China. *Water* **13**(14), 1900 (2021)
6. Reuter, D., et al.: The operational land imager (OLI) and the thermal infrared sensor (TIRS) on the Landsat data continuity mission (LDCM). In: Algorithms and Technologies for Multispectral, Hyperspectral, and Ultraspectral Imagery XVII 8048, pp. 382–388 (2011)
7. Liu, Q.Y., Yu, T., Zhang, W.H.: Validation of gaofen-1 satellite geometric products based on reference data. *J. Indian Soc. Remote Sens.* **47**(8), 1331–1346 (2019)
8. Zhu, Z., et al.: Continuous monitoring of land disturbance based on Landsat time series. *Remote Sens. Environ.* **238**, 111–116 (2020)
9. Xu, Z.H.: Parallel calculation method of patch area landscape art index based on surface coverage data. *Secur. Commun. Netw.* **2021**, 1–10 (2021)
10. Zhao, F., Li, H., Li, C.H., Cai, Y.P., Wang, X., Liu, Q.: Analyzing the influence of landscape pattern change on ecological water requirements in an arid/semiarid region of China. *J. Hydrol.* **578**, 124098 (2019)
11. Yeboah, D., Chen, H.Y.H., Kingston, S.: Tree species richness decreases while species evenness increases with disturbance frequency in a natural boreal forest landscape. *Ecol. Evol.* **6**(3), 842–850 (2016)
12. Wang, X.F., Zhou, C.W., Feng, X.M., Cheng, C.W., Fu, B.J.: Testing the efficiency of using high-resolution data from GF-1 in land cover classifications. *IEEE J. Sel. Top. Appl. Earth Observ. Remote Sens.* **11**(9), 3051–3061 (2018)